

# Radiative proton capture on ${}^6\text{He}$

E. Sauvan<sup>a\*</sup>, F.M. Marqués<sup>a†</sup>, H.W. Wilschut<sup>b</sup>, N.A. Orr<sup>a</sup>, J.C. Angélique<sup>a</sup>, C. Borcea<sup>c</sup>, W.N. Catford<sup>d</sup>, N.M. Clarke<sup>e</sup>, P. Descouvemont<sup>f</sup>, J. Díaz<sup>g</sup>, S. Grévy<sup>a</sup>, A. Kugler<sup>h</sup>, V. Kravchuk<sup>b</sup>, M. Labiche<sup>a‡</sup>, C. Le Brun<sup>a§</sup>, E. Lienard<sup>a</sup>, H. Löhner<sup>b</sup>, W. Mittig<sup>i</sup>, R.W. Ostendorf<sup>b</sup>, S. Pietri<sup>a</sup>, P. Roussel-Chomaz<sup>i</sup>, M.G. Saint Laurent<sup>i</sup>, H. Savajols<sup>i</sup>, V. Wagner<sup>h</sup>, N. Yahlali<sup>g</sup>

<sup>a</sup> *Laboratoire de Physique Corpusculaire, IN2P3-CNRS, ISMRA et Université de Caen, F-14050 Caen cedex, France*

<sup>b</sup> *Kernfysich Versneller Instituut, Zernikelaan 25, NL-9747 AA Groningen, The Netherlands*

<sup>c</sup> *IFIN-HH, P.O. Box MG-6, 76900 Bucharest-Magurele, Romania*

<sup>d</sup> *Department of Physics, University of Surrey, Guildford, Surrey, GU2 7XH, U.K.*

<sup>e</sup> *School of Physics and Astronomy, University of Birmingham, Birmingham B15 2TT, U.K.*

<sup>f</sup> *Université Libre de Bruxelles, CP 229, B-1050 Bruxelles, Belgium*

<sup>g</sup> *Instituto de Física Corpuscular, E-46100 Burjassot, Spain*

<sup>h</sup> *Nuclear Physics Institute, 25068 Řež u Prahy, Czech Republic*

<sup>i</sup> *GANIL, CEA/DSM-CNRS/IN2P3, BP 55027, F-14076 Caen cedex, France*

(November 10, 2018)

Radiative capture of protons is investigated as a probe of clustering in nuclei far from stability. The first such measurement on a halo nucleus is reported here for the reaction  ${}^6\text{He}(p,\gamma)$  at 40 MeV. Capture into  ${}^7\text{Li}$  is observed as the strongest channel. In addition, events have been recorded that may be described by quasi-free capture on a halo neutron, the  $\alpha$  core and  ${}^5\text{He}$ . The possibility of describing such events by capture into the continuum of  ${}^7\text{Li}$  is also discussed.

PACS number(s): 25.40.Lw, 25.10.+s, 21.45.+v

In the vicinity of the neutron drip-line, the weak binding of valence neutrons may lead to the formation of spatially extended nuclei [1]. The most exotic of these are the core-n-n halo systems,  ${}^6\text{He}$ ,  ${}^{11}\text{Li}$  and  ${}^{14}\text{Be}$ , which exhibit Borromean characteristics whereby the two-body subsystems are unbound [2]. Owing to the large cross sections, of the order of barns, dissociation reactions have been the most widely exploited method to study the internal correlations [3–5]. The task, however, in such an approach is complicated by the interplay of the reaction mechanism and final-state interactions (FSI) with the intrinsic structure [6]. The possibility of using the interference between 2n transfer and elastic scattering with  ${}^6\text{He}$  has also been considered [7,8].

Recently, an investigation of coherent bremsstrahlung production in the reaction  $\alpha(p,\gamma)$  at 50 MeV has demonstrated that the high-energy photon spectrum is dominated by capture to form  ${}^5\text{Li}$  [9]. Such results have motivated the extension of this technique to study  ${}^6\text{He}$ . Given a proton wavelength of  $\lambda = 0.7$  fm at 40 MeV, it may be possible to observe direct capture, as a quasi-free

process, on the constituents of  ${}^6\text{He}$  in addition to capture into  ${}^7\text{Li}$ . Moreover, the different quasi-free capture (QFC) processes would lead to different  $E_\gamma$  in the range 20–40 MeV. In this Letter the first experimental results for capture on a halo nucleus are reported. Evidence for QFC on  ${}^4,5\text{He}$  and n is presented; capture, however, on a di-neutron does not appear to occur. These observations suggest that radiative capture may provide a new probe for the study of clustering in the ground state (g.s.) of nuclei far from stability.

The  ${}^6\text{He}$  beam ( $5 \times 10^5$  pps,  $\Delta E/E \sim 1\%$ ) was produced by fragmentation of a  ${}^{13}\text{C}$  primary beam using the GANIL coupled cyclotron facility, and bombarded a solid Hydrogen target [10] with a thickness of  $95 \text{ mg/cm}^2$ ; the mean beam energy at the target midpoint was 40 MeV/N. The different charged reaction products emitted in the forward direction ( $\pm 2^\circ$ ) were identified, and momentum analysed, using the SPEG spectrometer [11], which covered a rigidity range of 1.45–1.85 Tm in three overlapping settings. The photons were detected in coincidence with the charged fragments using the “Château de Cristal” array, with the  $74 \text{ BaF}_2$  crystals placed around the target at a distance of 30 cm in two domes [12], the total efficiency being close to 70%. The energy calibration, in the range 1–100 MeV, was determined from the energy deposited by cosmic-ray muons [13] and the 4.43 MeV  $\gamma$ -rays from an Am-Be source. The energy and angle of the photons were reconstructed using a clustering algorithm [13,14], with average energy and angular resolutions of 17% and  $10^\circ$ , respectively. The event trigger required an energy deposition of at least 3 MeV in one crystal in coincidence with a fragment in SPEG. Owing to the compact geometry of the Château and the energy spread in the beam ( $\Delta t \sim 6$  ns at the target position), event-by-event  $\gamma$ -n discrimination was not possible. However, for each class of events the mean flight time between the  $\text{BaF}_2$  crystals and the accelerator RF signal ( $\langle t_{\text{BaF}} \rangle$ ) could be determined. A Monte-Carlo simulation was developed, in which the response of the Château and the conversion of photons in the tar-

\*Present address: ISOLDE, CERN, Switzerland.

†e-mail: Marqués@caelav.in2p3.fr

‡Present address: University of Paisley, Scotland.

§Present address: ISN, Grenoble, France.

get frame were simulated using GEANT [15]; the characteristics of the secondary beam and the spectrometer acceptances were also included [13].

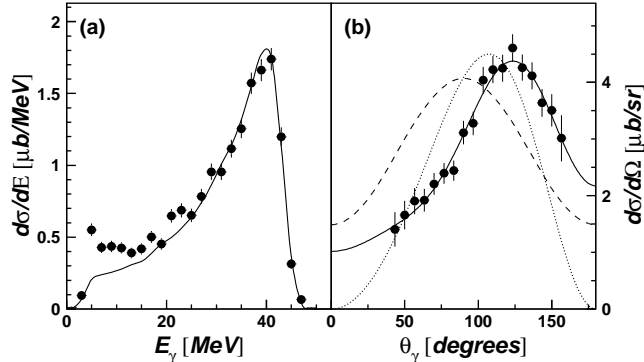


FIG. 1. Energy (a) and angular distributions (b) in the  ${}^6\text{He}+p$  c.m. for photons in coincidence with  ${}^7\text{Li}$ . The solid line in (a) is the response of the Chateau to  $E_\gamma = 42$  MeV. The lines in (b) correspond to a classical electrostatics calculation (dotted), a microscopic cluster model (dashed), both normalized to the data, and to a Legendre polynomial fit (solid).

Turning to the experimental observations, the capture reaction  ${}^6\text{He}(p,\gamma){}^7\text{Li}$  is unambiguously identified by the  $\gamma$ -rays in coincidence with  ${}^7\text{Li}$  (Fig. 1). In particular, the photon energy spectrum, as well as the  ${}^7\text{Li}$  momentum [13], is well described assuming a  $\gamma$ -ray line at 42 MeV and is free of background at higher energies. The two particle-stable states of  ${}^7\text{Li}$ , the g.s. and the first excited state at 0.48 MeV, were too close together in energy to be distinguished in this experiment. In addition, the lowest threshold on any of the  $\text{BaF}_2$  crystals, 1 MeV, prevented observation of the 0.48 MeV  $\gamma$ -ray. The photon angular distribution (Fig. 1b) is slightly backward peaked, as expected from classical electrostatics [16] due to the charge asymmetry of the entrance channel. A fit with a Legendre polynomial [17] leads to  $a_{i=1,4} = -0.57 \pm 0.10$ ,  $-0.28 \pm 0.13$ ,  $0.37 \pm 0.10$ ,  $-0.21 \pm 0.12$ , respectively. The total efficiency for the detection of  ${}^7\text{Li}-\gamma$  coincidences was estimated to be  $37 \pm 2\%$ , and the deduced cross section was  $\sigma = 35 \pm 2 \mu\text{b}$ . As only photons are liberated in this reaction, the measured time spectrum served as a reference,  $\langle t_\gamma \rangle$ , for other channels in which neutrons were also emitted.

The  ${}^6\text{He}(p,\gamma){}^7\text{Li}$  cross section has been calculated using a microscopic cluster model [18]. The  ${}^7\text{Li}$  and  ${}^6\text{He}+p$  wave functions were defined by antisymmetric products of cluster wave functions, including  ${}^6\text{He}+p$ ,  ${}^6\text{Li}+n$  and  $\alpha+t$  structures. Excited states of  ${}^6\text{He}$  and  ${}^6\text{Li}$  were included in the basis. The Minnesota interaction was used to specify the N-N force [19], with an exchange parameter  $u = 0.935$  and a zero-range spin-orbit force with amplitude  $S_0 = 38 \text{ MeVfm}^5$ . This model provides a good description of the cross sections at low energy for  $t(\alpha,\gamma){}^7\text{Li}$ ,  ${}^6\text{Li}(p,\gamma){}^7\text{Be}$  and  ${}^6\text{Li}(p,\alpha){}^3\text{He}$ . At 40 MeV, a cross section

for  ${}^6\text{He}(p,\gamma){}^7\text{Li}$  of  $\sigma = 59 \mu\text{b}$  is calculated, with  $15 \mu\text{b}$  going to the g.s. and  $44 \mu\text{b}$  to the first excited state. At high energy, the microscopic model is expected to provide an upper limit to the cross section as some open channels, such as three-body ones, are not included. The relative population  $\sigma_{0.48}/\sigma_{\text{g.s.}} = 2.9$  should, however, be more reliable. The calculation was restricted to the dominant E1 multipolarity, thus leading to an angular distribution symmetric about  $90^\circ$  (Fig. 1b). The cross section to the g.s. can be obtained from photodisintegration [20] via detailed balance considerations and is  $9.6 \pm 0.4 \mu\text{b}$ . Given the predicted relative populations of the ground and first excited state, a total capture cross section of  $\sigma \sim 38 \mu\text{b}$  is obtained, in agreement with the value measured here.

QFC has been investigated by searching for  $\gamma$ -rays in coincidence with fragments lighter than  ${}^7\text{Li}$ . The corresponding energy spectra (Fig. 2a,c,e) do indeed exhibit peaks below 42 MeV. In order to establish the origin of these fragment- $\gamma$  coincidences, QFC processes on the subsystems of  ${}^6\text{He}$  have been modelled as follows. The  ${}^6\text{He}$  projectile is considered as a cluster (A) plus spectator (a) system in which each component has an intrinsic momentum distribution, the corresponding energy  $E_A + E_a - m_{{}^6\text{He}}$  being taken into account in the total available energy. The reaction may be denoted as  $a+A(p,\gamma)B+a$ , and the  $\gamma$ -ray angular distribution is assumed to be that given by the charge asymmetry of the entrance channel (A+p) [16]. The intrinsic momentum distribution of all the clusters was taken to be Gaussian in form with  $\text{FWHM} = 80 \text{ MeV}/c$  [13]; the resolution in the measured photon energy is such that the results are relatively insensitive to the exact value.

In order to explore the possibility that FSI may occur in the exit channel between the spectator,  $a$ , and the capture fragment,  $B$ , an extended version of the QFC calculation was developed. Here the energy available in the system  $B+a$  is treated as an excitation in the continuum of  ${}^7\text{Li}$ , which is allowed to decay in flight.

In the case of  ${}^6\text{Li}-\gamma$  coincidences, two lines were observed (Fig. 2a) at 30 and 3.5 MeV. These are clearly associated with the formation of  ${}^6\text{Li}$  and the decay of the second excited state, at 3.56 MeV [21]. Taking into account the detection efficiencies, we find that the  ${}^6\text{Li}$  is formed almost exclusively ( $96_{-24}^{+4}\%$ ) in the 3.56 MeV excited state. The estimated cross section was  $\sigma = 3.5 \pm 1.3 \mu\text{b}$ . The lines in Fig. 2a,b represent the results of QFC on  ${}^5\text{He}$  into  ${}^6\text{Li}^*(3.56 \text{ MeV})$ . The  $\gamma$ -ray energy spectrum is well described, while reproducing the  ${}^6\text{Li}$  momentum distribution requires inclusion of  ${}^6\text{Li}-n$  FSI as described above. The QFC with fragment FSI approach is thus the one employed in the following discussions.

The apparently exclusive population of the  ${}^6\text{Li}^*(3.56 \text{ MeV})$  indicates the importance of this state as the  $T = 1$  analogue of  ${}^6\text{He}_{\text{g.s.}}$ . It has been shown that the configuration of the 3.56 MeV state is likely to be “a spatially extended halolike structure formed by the neutron and proton outside the  $\alpha$  particle” [22], possibly even more extended than  ${}^6\text{He}$ . In terms of the QFC process the

population of this state is greatly favoured owing to the overlap of the initial and final wave functions. In the case of capture on  ${}^6\text{He}$  into the  ${}^7\text{Li}$  continuum, the reaction can proceed via the  $T = 3/2$  state at 11.24 MeV [21] (the  $T_{3/2}^+$  state of  ${}^7\text{Li}_{\text{g.s.}}$ ), which can only decay by neutron emission to a  $T = 1$  state in  ${}^6\text{Li}$ . Note, however, that the 11.24 MeV state in  ${}^7\text{Li}$  can also be formed in the exit channel following QFC on  ${}^5\text{He}$ , as the distribution of  ${}^6\text{Li}$ -n relative energy (Fig. 3) is centered at  $\sim 12$  MeV.

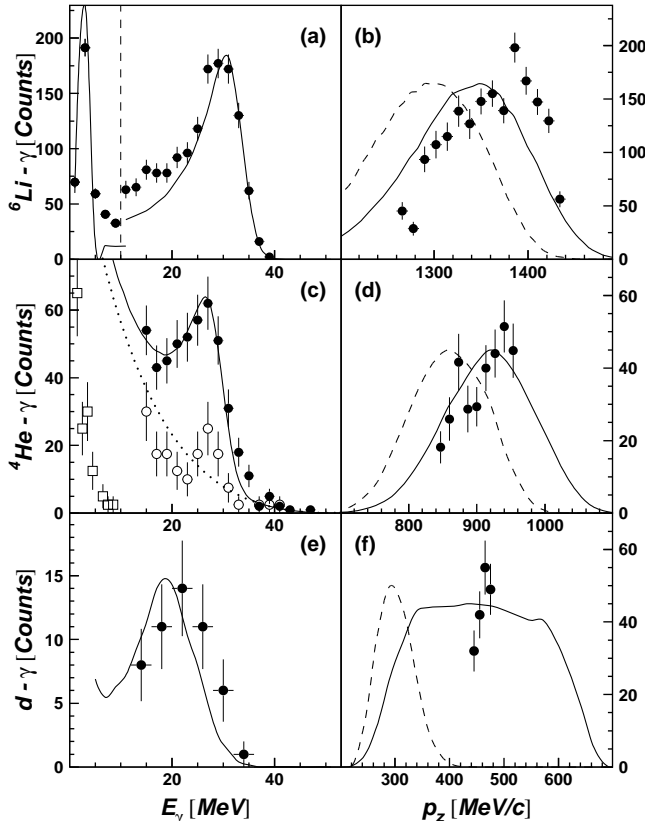


FIG. 2.  $\gamma$ -ray energy spectrum in the  ${}^6\text{He}+p$  c.m. and momentum distribution of the coincident fragment for  ${}^6\text{Li}$  (upper),  $\alpha$  particles (middle) and deuterons (lower panels). The lines correspond to calculations of QFC on the  ${}^5\text{He}$  cluster, the  $\alpha$  core and one halo neutron, respectively, on the right with/without (solid/dashed) fragment FSI (see text). The distribution in (a) was divided by 3 below 10 MeV, and the open symbols in (c) are from an analysis investigating the role of the neutron background (see text).

We have also searched for evidence of QFC on the  $\alpha$  core, whereby the two halo neutrons would behave as spectators. The photon spectrum should resemble that observed for the  $\alpha+p$  reaction [9]. Indeed such a  $\gamma$ -ray energy spectrum (Fig. 2c) has been observed in coincidence with  $\alpha$  particles. The background, however, arising from  ${}^6\text{He}$  breakup, in which the  $\alpha$  particle is detected in SPEG and the halo neutrons interact with the forward-angle detectors of the Chateau, is significant. In order to minimise this background, only the backward-angle

detectors ( $\theta > 110^\circ$ ) of the Chateau have been used in the analysis. The  $\gamma$ -ray spectrum under this condition exhibits two components: a peak at  $E_\gamma = 27$  MeV and a  $1/E_\gamma$  continuum similar to coherent  $\alpha+p$  bremsstrahlung [9].

Simulations indicate, however, that some back-scattered neutrons remain from breakup ( $\langle t_{\text{BaF}} \rangle - \langle t_\gamma \rangle = 0.8 \pm 0.1$  ns), which would also lead to a continuous component with a  $1/E$  type spectrum in the Chateau [13]. This would explain why the peak-to-continuum ratio is smaller here than that found in Ref. [9]. Therefore, we have added a single background component with a  $1/E$  form (dotted line in Fig. 2c) to the QFC process  $\alpha(p,\gamma){}^5\text{Li}$ . The photon energy spectrum is thus well described, as is the momentum distribution of the  $\alpha$  particle. The cross section is estimated to be  $\sigma = 4 \pm 1 \mu\text{b}$ . Additional support may be found in  $\alpha$ - $\gamma$ -n coincidences, for which some 30 events are observed. Here, the neutron was associated with events in the forward-angle detectors ( $\theta < 60^\circ$ ,  $\langle t_{\text{BaF}} \rangle - \langle t_\gamma \rangle = 5 \pm 4$  ns) and the photon with events observed in coincidence at backward angles ( $\theta > 110^\circ$ ,  $\langle t_{\text{BaF}} \rangle - \langle t_\gamma \rangle = 1.6 \pm 1.4$  ns). The resulting spectra exhibit the  $1/E$  form for neutrons (open squares) and, more importantly, a higher peak-to-continuum signal at 27 MeV for the photons (open circles) which is closer to that measured previously for the  $\alpha(p,\gamma){}^5\text{Li}$  reaction [9].

Finally, d- $\gamma$  coincidences presenting a peak in the  $\gamma$ -ray energy spectrum, at  $E_\gamma = 20$ –22 MeV, were also observed (Fig. 2e). For this channel the analysis was also restricted to the backward-angle detectors ( $\theta > 110^\circ$ ) of the Chateau. The relatively low statistics arise from the limited acceptances of the spectrometer for deuterons (Fig. 2f). We have verified with an empty-target run that no background events are present in the energy range in question, and that the events observed correspond to photons ( $\langle t_{\text{BaF}} \rangle - \langle t_\gamma \rangle = 0.0 \pm 0.3$  ns). The predictions for  $n(p,\gamma)d$  QFC on one halo neutron present a peak at 19 MeV (Fig. 2f). The small shift may be attributable to the strong kinematic correlation between the deuteron momentum and the photon energy, as the detection of a very small fraction of the deuterons (depending on the neutron momentum distribution used) is predicted [13]. Given these uncertainties, no reliable estimate of the cross section for this channel was possible.

There are additional QFC channels,  $2n(p,\gamma)t$  and  $t(p,\gamma)\alpha$ , that could have been observed with finite efficiency in this experiment but were not [13]. Perhaps the most interesting is QFC on the two halo neutrons. In the case of  ${}^6\text{He}$ , several theoretical models predict the coexistence of two configurations in the g.s. wave function: the so-called “di-neutron” and “cigar” configurations [2]. Here one might expect that the different admixtures of these could be probed by the relative strength of the  $n, 2n(p,\gamma)d, t$  QFC processes, whereby the corresponding free cross sections at 40 MeV, obtained from detailed balance considerations, are comparable:  $9.6 \mu\text{b}$  [23] and  $9.8 \mu\text{b}$  [24], respectively. However, events registered in

the Château in coincidence with tritons in SPEG have energies below 10 MeV, whereas the  $2n(p,\gamma)t$  reaction should produce photons with  $E_\gamma \approx 32$  MeV. In addition, the flight time  $\langle t_{\text{BaF}} \rangle - \langle t_\gamma \rangle = 4.7 \pm 0.2$  ns clearly corresponded to neutrons.

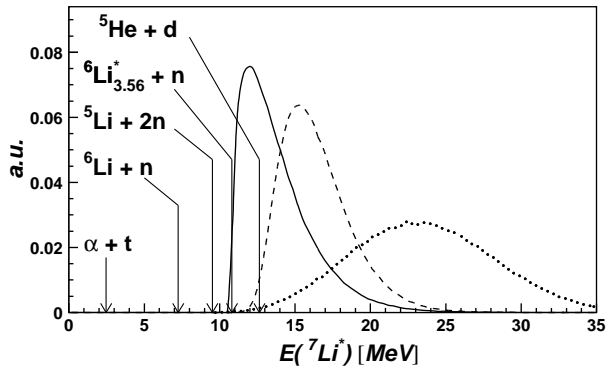


FIG. 3. Relative energies within the QFC with FSI model (see text) of the fragments in the exit channel following capture on  ${}^5\text{He}$ , the  $\alpha$  core and halo neutrons (solid, dashed and dotted lines, respectively). The various decay thresholds in  ${}^7\text{Li}$  are indicated by the arrows.

We have seen that the QFC with fragment FSI model describes well the monoenergetic  $\gamma$ -rays observed, as well as the momentum distribution of the capture fragment ( $B$ ). The  $\gamma$ -ray lines are associated with *specific* energy distributions for the fragments in the exit channel (Fig. 3), depending on the intrinsic momenta of the clusters. Therefore, such a process will exhibit the same kinematics as capture into continuum states above the corresponding threshold,  ${}^6\text{He}(p,\gamma){}^7\text{Li}^* \rightarrow B+a$ , provided that the equivalent region of the continuum (Fig. 3) is populated. If, however, all the final states observed here were the result of radiative capture into  ${}^7\text{Li}$ , capture via the non-resonant continuum in  ${}^7\text{Li}$  might well be expected to occur [25]. This would lead to a continuous component to the  $\gamma$ -ray energy spectra. Moreover, events corresponding to  $E_{7\text{Li}^*} = 0.5\text{--}10$  MeV have not been observed in either  $t$ - $\gamma$  coincidences or  $\alpha$ - $\gamma$  coincidences with  $E_\gamma = 32\text{--}42$  MeV, nor has the decay into  $\alpha+t$  for  $E_{7\text{Li}^*} > 10$  MeV. Within the picture of QFC on clusters, this is simply explained by the absence of the  $2n(p,\gamma)t$  and  $t(p,\gamma)\alpha$  QFC processes for the  ${}^4\text{He}$ - $2n$  [2] and  $t$ - $t$  [26] configurations, respectively, indicating that  ${}^4\text{He}$ - $n$ - $n$  is the dominant configuration in  ${}^6\text{He}$ . This in agreement with the relatively large  $n$ - $n$  distance found in Ref. [6].

In summary, radiative capture of protons on a halo nucleus,  ${}^6\text{He}$ , has been measured for the first time. In addition to the  ${}^6\text{He}(p,\gamma){}^7\text{Li}$  reaction, evidence for QFC on subsystems ( ${}^5\text{He}$ ,  $\alpha$  and  $n$ ) of  ${}^6\text{He}$  has been found. Of particular importance is the observation of events which correspond to the previously measured  $\alpha(p,\gamma)$  reaction, as well as the non-observation of capture on a di-neutron. Theoretically, microscopic models need to be developed in order to describe capture on the constituent clusters

of exotic nuclei and, for comparison, capture on the projectile into unbound final states. In this context, better knowledge of the high-lying continuum of  ${}^7\text{Li}$  would be very helpful. Finally, it would be of interest to study the evolution with beam energy of the contribution of QFC on clusters.

The support provided by the technical and operations staff of GANIL and LPC-Caen is gratefully acknowledged. Additional support from the Human Capital and Mobility Programme of the European Community (contract n $^\circ$  CHGE-CT94-0056) and the GDR Noyaux Exotiques (CNRS-CEA) is also acknowledged.

- 
- [1] P.G. Hansen, A.S. Jensen and B. Jonson, *Ann. Rev. Nucl. Part. Sci.* **45**, 591 (1995).
  - [2] M.V. Zhukov *et al.*, *Phys. Rep.* **231**, 151 (1993).
  - [3] D. Sackett *et al.*, *Phys. Rev. C* **48**, 118 (1993).
  - [4] M. Zinser *et al.*, *Nucl. Phys. A* **619**, 151 (1997).
  - [5] T. Aumann *et al.*, *Phys. Rev. C* **59**, 1252 (1999).
  - [6] F.M. Marqués *et al.*, *Phys. Lett. B* **476**, 219 (2000).
  - [7] Yu.Ts. Oganessian, V.I. Zagrebaev, J.S. Vaagen, *Phys. Rev. Lett.* **82**, 4996 (1999).
  - [8] I.V. Krouglov and W. von Oertzen, *Eur. Phys. J. A* **8**, 501 (2000).
  - [9] M. Hoefman *et al.*, *Phys. Rev. Lett.* **85**, 1404 (2000).
  - [10] J.F. Libin, P. Gangnant, GANIL Report, Aires 10/97 (1997).
  - [11] L. Bianchi *et al.*, *Nucl. Instr. and Meth. A* **276**, 509 (1989).
  - [12] H. Ejiri, M.J.A. de Voigt, *Gamma-Ray and Electron Spectroscopy in Nuclear Physics*, Clarendon Press, Oxford, p144 (1989).
  - [13] E. Sauvan, Thèse, Université de Caen, LPCC T-00-01 (2000); E. Sauvan *et al.*, in preparation.
  - [14] F.M. Marqués *et al.*, *Nucl. Instr. and Meth. A* **365**, 392 (1995).
  - [15] R. Brun *et al.*, Technical Report CERN/DD/EE/84 (1997).
  - [16] M. Hoefman *et al.*, *Nucl. Phys. A* **654**, 779c (1999).
  - [17] H.R. Weller *et al.*, *Phys. Rev. C* **25**, 2921 (1982).
  - [18] P. Descouvemont, *Nucl. Phys. A* **584**, 532 (1995).
  - [19] D.R. Thompson, M. LeMere, Y.C. Tang, *Nucl. Phys. A* **286**, 53 (1977).
  - [20] M.R. Sené *et al.*, *Nucl. Phys. A* **442**, 215 (1985).
  - [21] F. Ajzenberg-Selove, *Nucl. Phys. A* **490**, 1 (1988).
  - [22] K. Arai, Y. Suzuki, K. Varga, *Phys. Rev. C* **51**, 2488 (1995); B.V. Danilin *et al.*, *Phys. Rev. C* **43**, 2835 (1991).
  - [23] J. Ahrens *et al.*, *Phys. Lett.* **52B**, 49 (1974).
  - [24] D.D. Faul *et al.*, *Phys. Rev. Lett.* **44**, 129 (1980).
  - [25] S.A. Siddiqui, N. Dytlewski, H.H. Thies, *Nucl. Phys. A* **458**, 387 (1986).
  - [26] K. Arai, Y. Suzuki, R.G. Lovas, *Phys. Rev. C* **59**, 1432 (1999).